

TD-CFIE Formulation for Transient Electromagnetic Scattering from 3-D Dielectric Objects

Young-Hwan Lee, Baek Ho Jung, Tapan K. Sarkar, Mengtao Yuan, Zhong Ji, and Seong-Ook Park

In this paper, we present a time domain combined field integral equation formulation (TD-CFIE) to analyze the transient electromagnetic response from dielectric objects. The solution method is based on the method of moments which involves separate spatial and temporal testing procedures. A set of the RWG functions is used for spatial expansion of the equivalent electric and magnetic current densities, and a combination of RWG and its orthogonal component is used for spatial testing. The time domain unknowns are approximated by a set of orthonormal basis functions derived from the Laguerre polynomials. These basis functions are also used for temporal testing. Use of this temporal expansion function characterizing the time variable makes it possible to handle the time derivative terms in the integral equation and decouples the space-time continuum in an analytic fashion. Numerical results computed by the proposed formulation are compared with the solutions of the frequency domain combined field integral equation.

Keywords: Transient, electromagnetic scattering, dielectric, CFIE, Laguerre polynomial.

Manuscript received Aug. 25, 2006; revised Dec. 11, 2006.

This work was supported by the Korean Research Foundation Grant (KRF-2004-041-D00302).

Young-Hwan Lee (phone: + 82 42 860 6572, email: yhwan@etri.re.kr) is with IT Technology Transfer Evaluation Center, ETRI, Daejeon, Korea.

Baek Ho Jung (email: bhjung@hoseo.edu) is with the Department of Information and Communication Engineering, Hoseo University, Chungnam, Korea.

Tapan Kumar Sarkar (email: tksarkar@syr.edu) is with the Department of Electrical and Computer Engineering, Syracuse University, NY, USA.

Mengtao Yuan (email: myuan@cadence.com) is with Cadence Design Systems Inc., Tempe, Arizona, USA.

Zhong Ji (email: zhong.ji@centurion.com) is with Laird Technologies, Lincoln, NE, USA.

Seong-Ook Park (email: sopark@jcu.ac.kr) is with the School of Engineering, Information and Communications University, Daejeon, Korea.

I. Introduction

The marching-on in time (MOT) technique is extensively employed to analyze the transient scattering from conducting and dielectric objects using time domain integral equations [1]. A serious drawback of this algorithm is the occurrence of late-time instabilities in the form of high frequency oscillation. Several MOT formulations have been presented for the solution of the electromagnetic scattering from arbitrarily shaped 3-D dielectric structures using triangular patch modeling techniques [2]-[4]. An explicit solution of the time domain formulation has been presented which differentiates the coupled integral equations using the MOT technique with second-order finite difference [2], but the results become unstable for late times. The late-time oscillations could be eliminated by approximating the average value of the current. In addition, a backward finite difference approximation for the magnetic vector potential term in the time domain electric field integral equation has been used for the implicit MOT technique to minimize these late-time oscillations [3], [4]. In spite of using an implicit technique to solve the time domain combined field integral equation (TD-CFIE) for the dielectric body, the solution obtained by using the MOT method still has late-time oscillation, which is dependent on the choice of the time step and the size of the structure to be considered.

In this paper, we present a new TD-CFIE formulation to obtain stable transient electromagnetic responses from arbitrarily shaped 3-D dielectric objects based on our recent work [5], which employed the PMCHW integral equation. The solution method in this paper is based on the method of moments (MoM) which involves separate spatial and temporal testing procedures. A set of the RWG functions is used for spatial expansion of the equivalent electric and magnetic

current densities and a combination of RWG and $\mathbf{n} \times \text{RWG}$ function with testing coefficients is used for spatial testing [6], [7]. Here, \mathbf{n} is the unit normally pointing outward from the surface at \mathbf{r} . We also investigate spatial testing procedures for the TD-CFIE to select the proper testing function set. The time domain unknowns are approximated by a set of orthogonal basis functions that are derived from the Laguerre polynomials [8]. The Laguerre series is defined only over the interval from zero to infinity, and hence, are considered to be more suited for the transient problem, as they naturally enforce causality. The temporal basis functions used in this work are completely convergent to zero as time increases to infinity. Therefore, the transient response spanned by these basis functions is also convergent to zero as time progresses. Using Galerkin's method, we introduce a temporal testing procedure, which is similar to the spatial testing procedure of the MoM. By applying temporal testing to the time domain integral equations, we can eliminate the numerical instabilities. Instead of the MOT procedure, we employ a marching-on in degree procedure by increasing the degree of the temporal testing functions. Therefore, we can obtain the unknown coefficients of the expansion by solving a matrix equation recursively with a finite number of basis functions. In the next section, we describe the integral equations. In section III, we set up a matrix equation by applying the MoM with spatial and temporal testing procedures. Section IV presents and compares numerical results followed by section V, the conclusion.

II. Integral Equations

In this section, we discuss the TD-CFIE formulation for a dielectric scatterer, which is illuminated by an electromagnetic pulse. We consider a homogeneous dielectric body with permittivity ϵ_2 and permeability μ_2 placed in an infinite homogeneous medium with permittivity ϵ_1 and permeability μ_1 as shown in Fig. 1.

By invoking the equivalence principle, the integral equation is formulated in terms of the equivalent electric and magnetic current densities \mathbf{J} and \mathbf{M} on surface S of the dielectric body. By enforcing the continuity of the tangential electric and

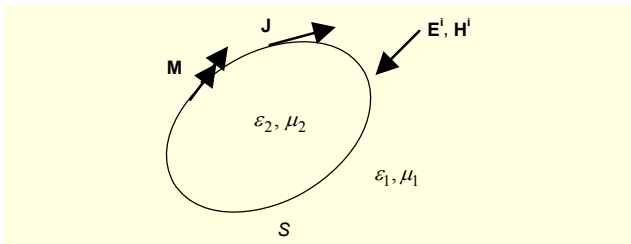


Fig. 1. Homogeneous dielectric body illuminated by an electromagnetic pulse.

magnetic fields at S , the following integral equations are obtained:

$$[-\mathbf{E}_v^s(\mathbf{r}, t)]_{\text{tan}} = \begin{cases} [\mathbf{E}^i(\mathbf{r}, t)]_{\text{tan}}, & v = 1, \mathbf{r} \in S, \\ 0, & v = 2, \mathbf{r} \in S, \end{cases} \quad (1)$$

$$[-\mathbf{H}_v^s(\mathbf{r}, t)]_{\text{tan}} = \begin{cases} [\mathbf{H}^i(\mathbf{r}, t)]_{\text{tan}}, & v = 1, \mathbf{r} \in S, \\ 0, & v = 2, \mathbf{r} \in S, \end{cases} \quad (2)$$

where \mathbf{E}^i and \mathbf{H}^i are the incident electric and magnetic fields, respectively. The subscript 'tan' denotes the tangential component. The scattered electric and magnetic fields are given by

$$\mathbf{E}_v^s(\mathbf{r}, t) = -\frac{\partial}{\partial t} \mathbf{A}_v(\mathbf{r}, t) - \nabla \Phi_v(\mathbf{r}, t) - \frac{1}{\epsilon_v} \nabla \times \mathbf{F}_v(\mathbf{r}, t), \quad (3)$$

$$\mathbf{H}_v^s(\mathbf{r}, t) = -\frac{\partial}{\partial t} \mathbf{F}_v(\mathbf{r}, t) - \nabla \Psi_v(\mathbf{r}, t) + \frac{1}{\mu_v} \nabla \times \mathbf{A}_v(\mathbf{r}, t). \quad (4)$$

In (3) and (4), \mathbf{A}_v and \mathbf{F}_v are the magnetic and electric vector potentials, and Φ_v and Ψ_v are the electric and magnetic scalar potentials given by

$$\mathbf{A}_v(\mathbf{r}, t) = \frac{\mu_v}{4\pi} \int_S \frac{\mathbf{J}(\mathbf{r}', \tau_v)}{R} dS', \quad (5)$$

$$\mathbf{F}_v(\mathbf{r}, t) = \frac{\epsilon_v}{4\pi} \int_S \frac{\mathbf{M}(\mathbf{r}', \tau_v)}{R} dS', \quad (6)$$

$$\Phi_v(\mathbf{r}, t) = \frac{1}{4\pi\epsilon_v} \int_S \frac{q_e(\mathbf{r}', \tau_v)}{R} dS', \quad (7)$$

$$\Psi_v(\mathbf{r}, t) = \frac{1}{4\pi\mu_v} \int_S \frac{q_m(\mathbf{r}', \tau_v)}{R} dS', \quad (8)$$

where $R = |\mathbf{r} - \mathbf{r}'|$ represents the distance between the arbitrarily located observation point \mathbf{r} and the source point \mathbf{r}' , $\tau_v = t - R/c_v$ is the retarded time, and $c_v = 1/\sqrt{\epsilon_v\mu_v}$ is the velocity of propagation of the electromagnetic wave in the space with medium parameters (ϵ_v, μ_v) . The electric and magnetic surface charge densities q_e and q_m are related to the electric and magnetic current density by the equations of continuity such that

$$\nabla \cdot \mathbf{J}(\mathbf{r}, t) = -\frac{\partial}{\partial t} q_e(\mathbf{r}, t), \quad (9)$$

$$\nabla \cdot \mathbf{M}(\mathbf{r}, t) = -\frac{\partial}{\partial t} q_m(\mathbf{r}, t). \quad (10)$$

For the CFIE formulation, a set of two integral equations are

formed from the set (1) and (2) by using the following form [7]:

$$(1-\kappa)[-E_v^s(\mathbf{r},t)]_{\text{tan}} + \kappa\eta_v[-H_v^s(\mathbf{r},t)]_{\text{tan}} = \begin{cases} (1-\kappa)[E^i(\mathbf{r},t)]_{\text{tan}} + \kappa\eta_1[H^i(\mathbf{r},t)]_{\text{tan}}, & v=1, \\ 0, & v=2, \end{cases} \quad (11)$$

where κ is the usual combination parameter which can have any value between 0 and 1, and η_v is the wave impedance of region v .

III. Numerical Implementation

The surface of the dielectric structure to be analyzed is approximated by planar triangular patches. As in [9], we use the RWG function associated with the n -th common edge as the spatial basis function defined as

$$\mathbf{f}_n(\mathbf{r}) = \mathbf{f}_n^+(\mathbf{r}) + \mathbf{f}_n^-(\mathbf{r}), \quad (12-1)$$

$$\mathbf{f}_n^\pm(\mathbf{r}) = \begin{cases} \frac{l_n}{2A_n^\pm} \boldsymbol{\rho}_n^\pm, & \mathbf{r} \in T_n^\pm, \\ 0, & \mathbf{r} \notin T_n^\pm, \end{cases} \quad (12-2)$$

where l_n and A_n^\pm are the length of the edge and the area of triangle T_n^\pm . The position vector defined with respect to the free vertex of T_n^\pm is denoted by $\boldsymbol{\rho}_n^\pm$. In general, the electric current density \mathbf{J} and the magnetic current density \mathbf{M} on the dielectric structure may be approximated in terms of this spatial basis function as

$$\mathbf{J}(\mathbf{r}, t) = \sum_{n=1}^N J_n(t) \mathbf{f}_n(\mathbf{r}), \quad (13)$$

$$\mathbf{M}(\mathbf{r}, t) = \sum_{n=1}^N M_n(t) \mathbf{f}_n(\mathbf{r}), \quad (14)$$

where J_n and M_n are constants yet to be determined, and N is the number of edges on the surface for the triangulated model approximating the surface of the dielectric body.

When (7) and (8) are used in (3) and (4), we encounter time-integral terms which are due to (9) and (10). For convenience, and to avoid the computation of the time derivatives numerically, we evaluate the time derivative of the vector potential in (3) and (4) analytically. We use the following two source vectors \mathbf{e} and \mathbf{h} introduced in [5]:

$$\mathbf{J}(\mathbf{r}, t) = \frac{\partial}{\partial t} \mathbf{e}(\mathbf{r}, t), \quad (15)$$

$$\mathbf{M}(\mathbf{r}, t) = \frac{\partial}{\partial t} \mathbf{h}(\mathbf{r}, t), \quad (16)$$

where the relation between these source vectors and the charge

densities are given through

$$q_e(\mathbf{r}, t) = -\nabla \cdot \mathbf{e}(\mathbf{r}, t), \quad (17)$$

$$q_m(\mathbf{r}, t) = -\nabla \cdot \mathbf{h}(\mathbf{r}, t). \quad (18)$$

By using (12), we may expand the two source vectors as

$$\mathbf{e}(\mathbf{r}, t) = \sum_{n=1}^N e_n(t) \mathbf{f}_n(\mathbf{r}), \quad (19)$$

$$\mathbf{h}(\mathbf{r}, t) = \sum_{n=1}^N h_n(t) \mathbf{f}_n(\mathbf{r}), \quad (20)$$

where e_n and h_n are the time domain unknown coefficients to be determined.

The next step in the numerical implementation scheme is to develop a testing procedure to transform the operator equation (11) into a matrix equation using the MoM. In the CFIE formulation, we may use a combination of RWG and $\mathbf{n} \times \text{RWG}$ as the testing function to convert the CFIE into a matrix equation. The $\mathbf{n} \times \text{RWG}$ function is associated with the n -th common edge, which is defined through

$$\mathbf{g}_n(\mathbf{r}) = \mathbf{g}_n^+(\mathbf{r}) + \mathbf{g}_n^-(\mathbf{r}), \quad (21-1)$$

$$\mathbf{g}_n^\pm(\mathbf{r}) = \mathbf{n} \times \mathbf{f}_n^\pm(\mathbf{r}). \quad (21-2)$$

The functions \mathbf{f}_n and \mathbf{g}_n are point-wise orthogonal in the triangle pair. A general expression for the testing of CFIE in the frequency domain using the four parameters in conjunction with the testing functions has been presented in [7]. By applying this testing procedure, we may write (11) as

$$(1-\kappa) \langle f_E \mathbf{f}_m + g_E \mathbf{g}_m, -E_v^s(\mathbf{r},t) \rangle + \kappa\eta_v \langle f_H \mathbf{f}_m + g_H \mathbf{g}_m, -H_v^s(\mathbf{r},t) \rangle = \begin{cases} (1-\kappa) \langle f_E \mathbf{f}_m + g_E \mathbf{g}_m, E^i(\mathbf{r},t) \rangle \\ \quad + \kappa\eta_1 \langle f_H \mathbf{f}_m + g_H \mathbf{g}_m, H^i(\mathbf{r},t) \rangle, & v=1, \\ 0, & v=2, \end{cases} \quad (22)$$

where $m=1, 2, \dots, N$ and the testing coefficients f_E, g_E, f_H and g_H may be +1 or -1. This equation is termed as the TENE-THNH formulation in [6]. TE is an abbreviation which means testing the electric field using \mathbf{f}_m as the testing function (short for $\mathbf{t} \cdot \mathbf{E}$ where \mathbf{t} denotes a unit vector tangential to S). Similarly, TH stands for testing the magnetic field using \mathbf{f}_m (short for $\mathbf{t} \cdot \mathbf{H}$). The abbreviations NE and NH are obtained by taking the cross product of \mathbf{n} with electric and magnetic fields and then testing by using \mathbf{f}_m , respectively [6].

To convert (22) into a matrix equation, we separate the CFIE into two categories: the electric field and the magnetic field parts. First, we test (1) in relation to the electric field only with $f_H \mathbf{f}_m + g_H \mathbf{g}_m$ as the testing function, yielding

$$\begin{aligned} & \sum_{n=1}^N \sum_{p,q} \left[\mu_v A_{mn}^{pq} \frac{d^2}{dt^2} e_n(\tau_{mn,v}^{pq}) + \frac{F_{mn}^{pq}}{\varepsilon_v} e_n(\tau_{mn,v}^{pq}) + \frac{G_{mn}^{pq}}{c_v \varepsilon_v} \frac{d}{dt} e_n(\tau_{mn,v}^{pq}) \right] \\ & + \sum_{n=1}^N \left[C_{mn,v} \frac{d}{dt} h_n(t) + \sum_{p,q} \left\{ \frac{D_{mn}^{pq}}{c_v} \frac{d^2}{dt^2} h_n(\tau_{mn,v}^{pq}) + E_{mn}^{pq} \frac{d}{dt} h_n(\tau_{mn,v}^{pq}) \right\} \right] \\ & = V_m^{E(v)}(t). \end{aligned} \quad (23)$$

This equation is termed as the TENE formulation in [6]. The elements in (23) are given in the appendix. In deriving (23), we assumed that the functions dependent on the following variable do not change appreciably within a given triangular patch so that

$$\tau_v = t - \frac{R}{c_v} \rightarrow \tau_{mn,v}^{pq} = t - \frac{R_{mn}^{pq}}{c_v}, \quad R_{mn}^{pq} = |\mathbf{r}_m^{cp} - \mathbf{r}_n^{cq}|,$$

where p and q are + or -. The position vector of the center in triangle T_n^\pm is denoted by \mathbf{r}_n^{\pm} .

Now, we consider the choice of the temporal basis functions and the temporal testing procedure. An orthogonal basis function set can be derived from the Laguerre polynomials through the representation [8]

$$\phi_j(t) = e^{-t/2} L_j(t), \quad (24)$$

where L_j is the Laguerre polynomial of degree j [10]. The coefficients $e_n(t)$ and $h_n(t)$ introduced in (19) and (20), are assumed to be causal electromagnetic response functions for $t \geq 0$, and can be expanded using (24) as

$$e_n(t) = \sum_{j=0}^{\infty} e_{n,j} \phi_j(st), \quad (25)$$

$$h_n(t) = \sum_{j=0}^{\infty} h_{n,j} \phi_j(st), \quad (26)$$

where $e_{n,j}$ and $h_{n,j}$ are unknown coefficients, and s is a scaling factor. Using the orthogonality property of the temporal basis functions, the expressions for the first and second derivatives of (25) and (26) can be written explicitly using the time domain coefficient which is derived in [8].

We substitute the expressions for the basis functions (25) and (26) which represent the unknown together with their derivatives into (23). Performing temporal testing (multiplying by $\phi(st)$) and integrating from zero to infinity, we get the matrix equation

$$\begin{bmatrix} \alpha_{mn}^{E(1)} & \beta_{mn}^{E(1)} \\ \alpha_{mn}^{E(2)} & \beta_{mn}^{E(2)} \end{bmatrix} \begin{bmatrix} e_{n,i} \\ h_{n,i} \end{bmatrix} = \begin{bmatrix} \gamma_{m,i}^{E(1)} \\ \gamma_{m,i}^{E(2)} \end{bmatrix}, \quad (27)$$

where

$$\alpha_{mn}^{E(v)} = \sum_{p,q} \left(\frac{s^2 \mu_v A_{mn}^{pq}}{4} + \frac{F_{mn}^{pq}}{\varepsilon_v} + \frac{s G_{mn}^{pq}}{2 c_v \varepsilon_v} \right) \exp\left(-\frac{s R_{mn}^{pq}}{2 c_v}\right), \quad (28)$$

$$\beta_{mn}^{E(v)} = \frac{s C_{mn,v}}{2} + \sum_{p,q} \left(\frac{s^2 D_{mn}^{pq}}{4 c_v} + \frac{s E_{mn}^{pq}}{2} \right) \exp\left(-\frac{s R_{mn}^{pq}}{2 c_v}\right), \quad (29)$$

$$\gamma_{m,i}^{E(v)} = V_{m,i}^{E(v)} + P_{m,i}^{E(v)} + Q_{m,i}^{E(v)}, \quad (30)$$

$$V_{m,i}^{E(v)} = \int_0^\infty \phi_i(st) V_m^{E(v)}(t) d(st), \quad (31)$$

$$\begin{aligned} P_{m,i}^{E(v)} = & - \sum_{n=1}^N \sum_{p,q} \left[\left(\frac{s^2 \mu_v A_{mn}^{pq}}{4} + \frac{F_{mn}^{pq}}{\varepsilon_v} + \frac{s G_{mn}^{pq}}{2 c_v \varepsilon_v} \right) \sum_{j=0}^{i-1} e_{n,j} I_{ij} \left(\frac{s R_{mn}^{pq}}{c_v} \right) \right. \\ & + s^2 \mu_v A_{mn}^{pq} \sum_{j=0}^i \sum_{k=0}^{j-1} (j-k) e_{n,k} I_{ij} \left(\frac{s R_{mn}^{pq}}{c_v} \right) \\ & \left. + \frac{s G_{mn}^{pq}}{c_v \varepsilon_v} \sum_{j=0}^i \sum_{k=0}^{j-1} e_{n,k} I_{ij} \left(\frac{s R_{mn}^{pq}}{c_v} \right) \right], \end{aligned} \quad (32)$$

$$\begin{aligned} Q_{m,i}^{E(v)} = & - \sum_{n=1}^N \left[s C_{mn,v} \sum_{k=0}^{i-1} h_{n,k} + \sum_{p,q} \left\{ \left(\frac{s^2 D_{mn}^{pq}}{4 c_v} + \frac{s E_{mn}^{pq}}{2} \right) \sum_{j=0}^{i-1} h_{n,j} I_{ij} \left(\frac{s R_{mn}^{pq}}{c_v} \right) \right. \right. \\ & + s^2 \frac{D_{mn}^{pq}}{c_v} \sum_{j=0}^i \sum_{k=0}^{j-1} (j-k) h_{n,k} I_{ij} \left(\frac{s R_{mn}^{pq}}{c_v} \right) \\ & \left. \left. + s E_{mn}^{pq} \sum_{j=0}^i \sum_{k=0}^{j-1} h_{n,k} I_{ij} \left(\frac{s R_{mn}^{pq}}{c_v} \right) \right\} \right], \end{aligned} \quad (33)$$

$$I_{ij} \left(\frac{s R_{mn}^{pq}}{c_v} \right) = \phi_{i-j} \left(\frac{s R_{mn}^{pq}}{c_v} \right) - \phi_{i-j-1} \left(\frac{s R_{mn}^{pq}}{c_v} \right), \quad j \leq i. \quad (34)$$

A similar procedure to obtain (27) can be found in detail in [8].

Next, we may write a matrix equation from (2) related to the magnetic field only, with $f_H \mathbf{f}_m + g_H \mathbf{g}_m$ as the testing function. This equation is termed as the THNH formulation in [6]. Using a similar procedure to derive (27) from (1), or applying a duality theorem, we obtain

$$\begin{bmatrix} \beta_{mn}^{H(1)} & \alpha_{mn}^{H(1)} \\ \beta_{mn}^{H(2)} & \alpha_{mn}^{H(2)} \end{bmatrix} \begin{bmatrix} e_{n,i} \\ h_{n,i} \end{bmatrix} = \begin{bmatrix} \gamma_{m,i}^{H(1)} \\ \gamma_{m,i}^{H(2)} \end{bmatrix}, \quad (35)$$

where

$$\alpha_{mn}^{H(v)} = \sum_{p,q} \left(\frac{s^2 \varepsilon_v A_{mn}^{pq}}{4} + \frac{F_{mn}^{pq}}{\mu_v} + \frac{s G_{mn}^{pq}}{2c_v \mu_v} \right) \exp \left(-\frac{s R_{mn}^{pq}}{2c_v} \right), \quad (36)$$

$$\beta_{mn}^{H(v)} = - \left[\frac{s C_{mn,v}}{2} + \sum_{p,q} \left(\frac{s^2 D_{mn}^{pq}}{4c_v} + \frac{s E_{mn}^{pq}}{2} \right) \exp \left(-\frac{s R_{mn}^{pq}}{2c_v} \right) \right], \quad (37)$$

$$\gamma_{m,i}^{H(v)} = V_{m,i}^{H(v)} + P_{m,i}^{H(v)} + Q_{m,i}^{H(v)}, \quad (38)$$

$$V_{m,i}^{H(v)} = \int_0^\infty \phi_i(st) V_m^{H(v)}(t) d(st), \quad (39)$$

$$P_{m,i}^{H(v)} = - \sum_{n=1}^N \sum_{p,q} \left[\left(\frac{s^2 \varepsilon_v A_{mn}^{pq}}{4} + \frac{F_{mn}^{pq}}{\mu_v} + \frac{s G_{mn}^{pq}}{2c_v \mu_v} \right) \sum_{j=0}^{i-1} h_{n,j} I_{ij} \left(\frac{s R_{mn}^{pq}}{c_v} \right) \right. \\ \left. + s^2 \varepsilon_v A_{mn}^{pq} \sum_{j=0}^i \sum_{k=0}^{j-1} (j-k) h_{n,k} I_{ij} \left(\frac{s R_{mn}^{pq}}{c_v} \right) \right. \\ \left. + \frac{s G_{mn}^{pq}}{c_v \mu_v} \sum_{j=0}^i \sum_{k=0}^{j-1} h_{n,k} I_{ij} \left(\frac{s R_{mn}^{pq}}{c_v} \right) \right], \quad (40)$$

$$Q_{m,i}^{H(v)} = \sum_{n=1}^N \left[s C_{mn,v} \sum_{k=0}^{i-1} e_{n,k} \right. \\ \left. + \sum_{p,q} \left[\left(\frac{s^2 D_{mn}^{pq}}{4c_v} + \frac{s E_{mn}^{pq}}{2} \right) \sum_{j=0}^{i-1} e_{n,j} I_{ij} \left(\frac{s R_{mn}^{pq}}{c_v} \right) \right. \right. \\ \left. \left. + s^2 \frac{D_{mn}^{pq}}{c_v} \sum_{j=0}^i \sum_{k=0}^{j-1} (j-k) e_{n,k} I_{ij} \left(\frac{s R_{mn}^{pq}}{c_v} \right) \right. \right. \\ \left. \left. + s E_{mn}^{pq} \sum_{j=0}^i \sum_{k=0}^{j-1} e_{n,k} I_{ij} \left(\frac{s R_{mn}^{pq}}{c_v} \right) \right] \right]. \quad (41)$$

In the above equations, the spatial integral elements are obtained from (A1)-(A7) in the appendix by changing f_H and g_H instead of f_E and g_E , respectively. The term $V_m^{H(v)}$ in (39) is given as (A20) in the appendix.

We may rewrite the matrix equations (27) and (35), respectively, as

$$\begin{bmatrix} \alpha_{mn}^E \\ \alpha_{mn}^H \end{bmatrix} \begin{bmatrix} c_{n,i} \\ c_{n,i} \end{bmatrix} = \begin{bmatrix} \gamma_{m,i}^E \\ \gamma_{m,i}^H \end{bmatrix}, \quad (42)$$

$$\begin{bmatrix} \alpha_{mn}^E \\ \alpha_{mn}^H \end{bmatrix} \begin{bmatrix} c_{n,i} \\ c_{n,i} \end{bmatrix} = \begin{bmatrix} \gamma_{m,i}^E \\ \gamma_{m,i}^H \end{bmatrix}, \quad (43)$$

where $c_{n,i} = e_{mi}$ for $n=1, 2, \dots, N$ and $c_{n,i} = h_{ni}$ for $n=N+1, N+2, \dots, 2N$. Finally, by combining TENE and THNH given in (42) and (43), respectively, we have a matrix equation for the CFIE associated with (22) as

$$[\alpha_{mn}] [c_{n,i}] = [\gamma_{m,i}], \quad i = 0, 1, 2, \dots, \infty, \quad (44)$$

where

$$\alpha_{mn} = (1 - \kappa) \alpha_{mn}^E + \kappa \eta_v \alpha_{mn}^H, \\ \gamma_{m,i} = (1 - \kappa) \gamma_{m,i}^E + \kappa \eta_v \gamma_{m,i}^H.$$

By solving (44) in a marching-on in degree manner with M temporal basis functions, the electric and magnetic transient current coefficients are expressed using the relations (13)-(16), (19) and (20) with (25) and (26) [8]. To minimize the number of iterations, we first choose the scaling factor s according to the bandwidth of the input pulse. When we obtain $e_{n,i}$ and $h_{n,i}$, we can transfer them to $J_{n,i}$ and $M_{n,i}$, which are the coefficients of the currents \mathbf{J} and \mathbf{M} . Since \mathbf{J} and \mathbf{M} have finite energy, $J_{n,i}$ and $M_{n,i}$ will approach zero when i is large enough. We can adaptively choose the number of iterations M when the magnitudes of $J_{n,i}$ and $M_{n,i}$ are negligible. Once the equivalent currents on the dielectric scatterer have been determined, we can compute the far scattered fields. These fields may be thought of as the superposition of the fields due to the electric and magnetic currents. When we consider a signal with time duration T_f in the time domain, we note that the upper limit of the integral in (31) and (39) can be replaced by the time duration sT_f instead of infinity.

IV. Numerical Examples

We present the numerical results for 3-D dielectric scatterers with a relative permittivity $\varepsilon_r = 2$ placed in the free space. In this section, c and η mean the speed of the wave propagation and the wave impedance of the free space, respectively. The scatterers are illuminated by a Gaussian plane wave, in which the electromagnetic fields are given by

$$\mathbf{E}^i(\mathbf{r}, t) = \mathbf{E}_0 \frac{4}{\sqrt{\pi}T} e^{-r^2}, \quad \mathbf{H}^i(\mathbf{r}, t) = \frac{1}{\eta} \hat{\mathbf{k}} \times \mathbf{E}^i(\mathbf{r}, t), \quad (45)$$

where $\gamma = (4/T)(ct - ct_0 - \mathbf{r} \cdot \hat{\mathbf{k}})$, $\hat{\mathbf{k}}$ is the unit vector in the direction of the wave propagation, T is the pulse width of the Gaussian pulse in light meters (lm), and t_0 is a time delay which represents the time at which the pulse peaks at the origin. One light meter is the length of time taken by the electromagnetic wave to travel one meter in free space. In this work, the field is incident from $\phi = 0^\circ$ and $\theta = 0^\circ$ with $\hat{\mathbf{k}} = -\hat{\mathbf{z}}$, and $\mathbf{E}_0 = \hat{\mathbf{x}}$. In the numerical computation, we use a Gaussian pulse of $T=4$ lm and $ct_0=6$ lm. We set $s=0.9 \times 10^9$ and $M=40$. All the solutions computed by our presented method are compared with the inverse discrete Fourier transform (IDFT) of the solutions by the frequency domain combined integral equation (FD-CFIE) formulation described in [7] in the range of 0 to 500 MHz intervals with 128 samples. The shaded patches included in the figures

indicate the location of the current to be observed associated with the common edge. The far field solutions are θ - (or x -) components of the electric field taken along the backward direction (+ z axis) from the scatterers. We may use two kinds of the spatial testing functions for which the testing coefficients may be chosen as in [7]:

$$\langle \mathbf{f}_m + \mathbf{g}_m, \text{EFIE} \rangle + \langle -\mathbf{f}_m + \mathbf{g}_m, \text{MFIE} \rangle,$$

$$\langle \mathbf{f}_m - \mathbf{g}_m, \text{EFIE} \rangle + \langle \mathbf{f}_m + \mathbf{g}_m, \text{MFIE} \rangle.$$

These testing techniques yield the same solutions in our work. It has also been suggested to drop one of the testing terms, resulting in

$$f_E \langle \mathbf{f}_m, \text{EFIE} \rangle + g_E \langle \mathbf{g}_m, \text{EFIE} \rangle + f_H \langle \mathbf{f}_m, \text{MFIE} \rangle + g_H \langle \mathbf{g}_m, \text{MFIE} \rangle$$

as given in [6]. These formulations are named TENE-TH ($g_H=0$), TENE-NH ($f_H=0$), TE-THNH ($g_E=0$), and NE-THNH ($f_E=0$), depending on which term is omitted. Applying this scheme to our TD-CFIE formulation, we have sixteen possible cases of CFIE with different testing coefficients as in FD-CFIE [7]. But none of the sixteen formulations give valid solutions in the time domain. (When we apply the MOT technique to solve the TD-CFIE, all of the sixteen cases fail in our experience.) Numerical results are presented using the testing coefficients as $f_E=1$, $g_E=1$, $f_H=-1$, and $g_H=1$ with the combination parameter of $\kappa=0.5$.

As a first example, we consider a dielectric sphere with a radius of 0.5 m centered at the origin. This has a total of 528 patches and 792 edges. Figure 2 shows the transient response for the θ -directed electric current density at the shaded patch of the sphere ($\theta=90^\circ$ and $\phi=7.5^\circ$) computed by the presented method and compares it with the IDFT of a frequency domain solution. Figure 3 shows the transient response for the θ -directed

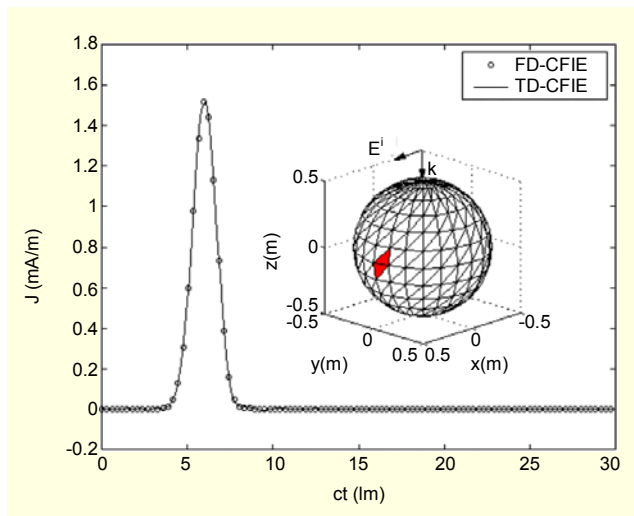


Fig. 2. Transient electric current density on the dielectric sphere.

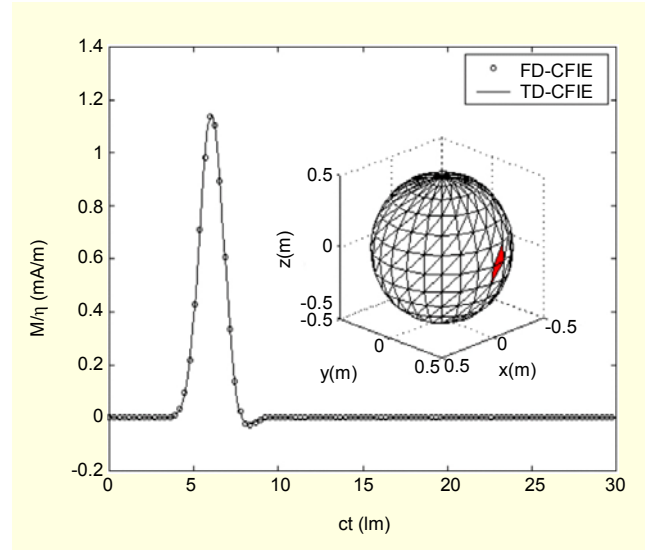


Fig. 3. Transient magnetic current density on the dielectric sphere.

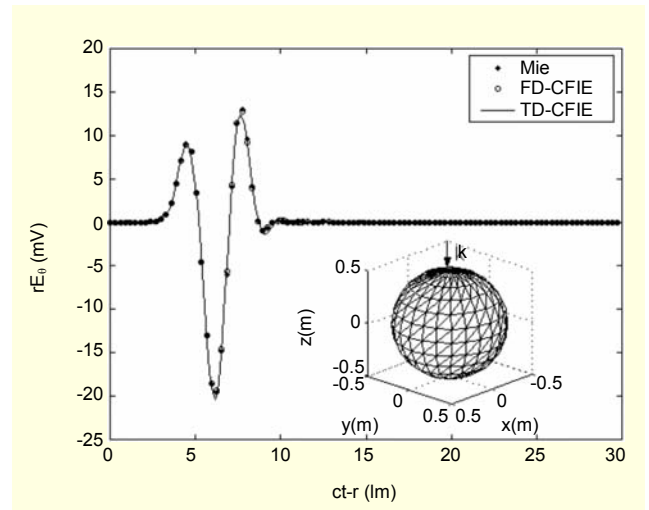


Fig. 4. Backward scattered field from the dielectric sphere along the + z direction.

magnetic current density at the shaded patch of the sphere ($\theta=90^\circ$ and $\phi=97.5^\circ$) computed by the present method and compares it with the IDFT solution. In Figs. 2 and 3, we can see that the solutions of the presented method are stable and the agreement with the IDFT solutions is good. Figure 4 presents the transient response for the backward scattered far field obtained by the technique just presented along with the Mie series solution and the IDFT solution. All three solutions agree well as is evident from the figure.

The next example is the dielectric structure of a hemisphere terminated by a cone. The radius of the hemisphere is 0.5 m and the height of the cone along the z -direction is 0.5 m. This structure is divided into 480 triangular patches with a total number of 720 edges. Figure 5 shows the transient response for

the θ -directed electric current density at the shaded patch on the hemisphere ($\theta=75^\circ$ and $\phi=7.5^\circ$) computed by the presented method and compares it with the IDFT solution. Figure 6 shows the transient response for the θ -directed magnetic current density at the shaded patch on the hemisphere ($\theta=75^\circ$ and $\phi=97.5^\circ$) computed by the present method and compares it with the IDFT solution. In Figs. 5 and 6, we can see that the solutions of the present method are stable and the agreement with the IDFT solutions is good. Figure 7 presents the transient response for the backward scattered far field from the dielectric hemisphere-cone obtained by the TD-CFIE along with the IDFT of the FD-CFIE solution. The two solutions agree well as is evident from the figure.

Finally, the structure of a dielectric double cones is considered,

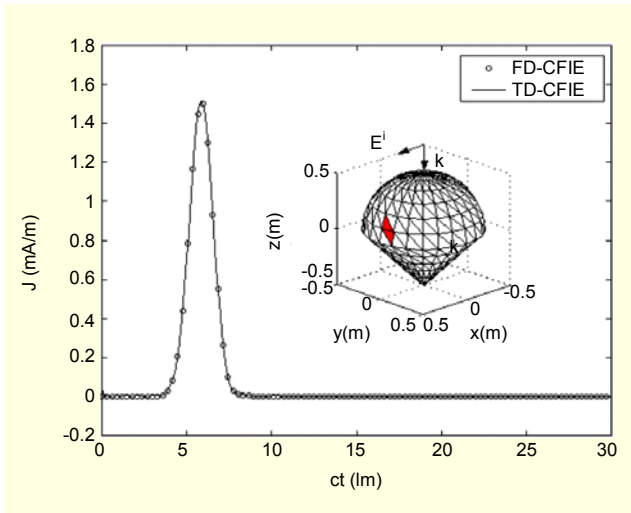


Fig. 5. Transient electric current density on the dielectric hemisphere-cone.

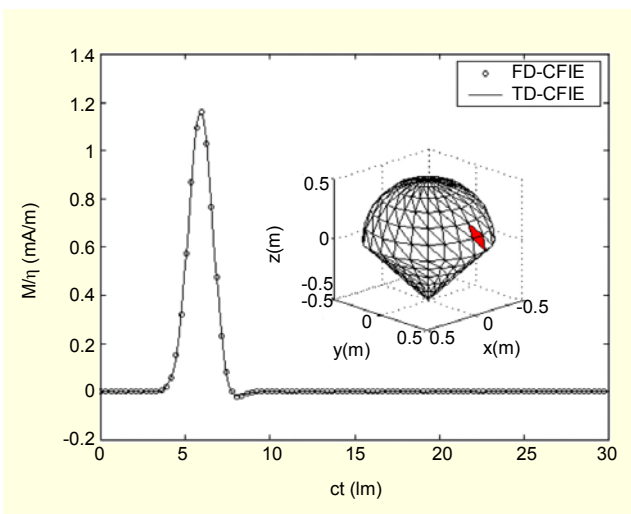


Fig. 6. Transient magnetic current density on the dielectric hemisphere-cone.

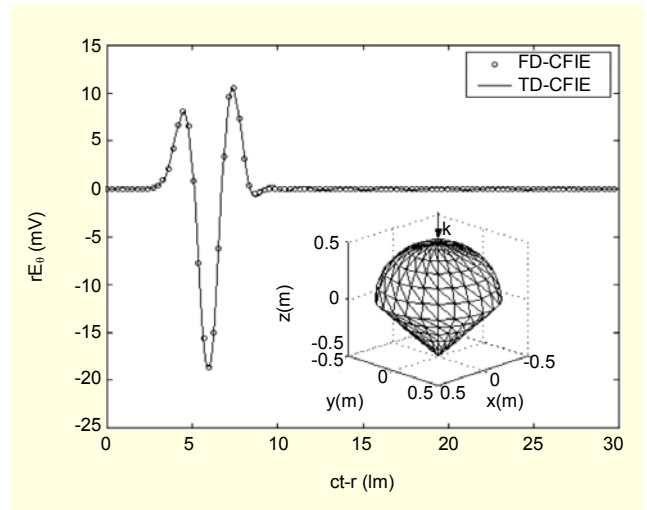


Fig. 7. Backward scattered field from the dielectric hemisphere-cone along the $+z$ direction.

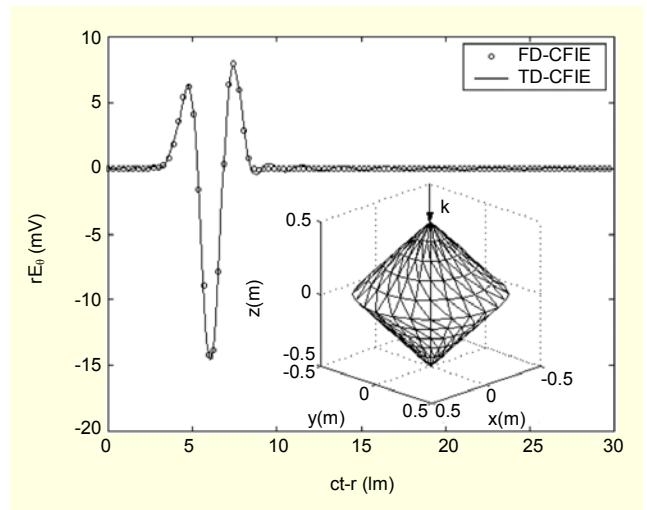


Fig. 8. Backward scattered field from the dielectric double cones along the $+z$ direction.

which is shown in Fig. 8. The height of the cones along the z -direction is 1 m and the radius at $z = 0$ is 0.5 m. This structure is divided into 432 triangular patches with a total number of 648 edges. In this figure, the backward scattered field computed by our proposed method is compared with the IDFT result. The agreement of the solution computed by the TD-CFIE and the IDFT of the FD-CFIE solution is excellent.

V. Conclusion

We have presented a novel method to solve the TD-CFIE for scattering from three-dimensional arbitrarily shaped dielectric structures. To apply an MoM procedure, we used the RWG vector function as the spatial basis function and a combination

of RWG and $\mathbf{n} \times \text{RWG}$ function for spatial testing. We introduced a temporal basis function set derived from the Laguerre polynomials and exponential functions. With the representation of the derivative of the transient coefficient in an analytic form, the temporal derivative in the integral equation can be treated analytically. Transient equivalent currents and far field obtained by the method presented in this paper are accurate and stable. We found that two kinds of testing techniques work. However, any of the formulations, which omit one of the testing terms, do not yield a valid solution for the TD-CFIE. The agreement between the solutions obtained using the proposed method and the IDFT of the frequency domain solution is excellent.

Appendix

Elements in (23) for the TENE formulation are given as

$$A_{mn}^{pq} = f_E a_{mn,f}^{pq} + g_E a_{mn,g}^{pq}, \quad (\text{A1})$$

$$F_{mn}^{pq} = f_E b_{mn,f}^{pq} + g_E g_{mn,g}^{pq}, \quad (\text{A2})$$

$$G_{mn}^{pq} = g_E f_{mn,g}^{pq}, \quad (\text{A3})$$

$$C_{mn,v} = \begin{cases} +C_{mn}, & v=1, \\ -C_{mn}, & v=2, \end{cases} \quad (\text{A4})$$

$$C_{mn} = \sum_{p,q} (f_E c_{mn,f}^{pq} + g_E c_{mn,g}^{pq}), \quad (\text{A5})$$

$$D_{mn}^{pq} = f_E d_{mn,f}^{pq} + g_E d_{mn,g}^{pq}, \quad (\text{A6})$$

$$E_{mn}^{pq} = f_E e_{mn,f}^{pq} + g_E e_{mn,g}^{pq}. \quad (\text{A7})$$

For the THNH formulation, the elements are obtained by changing f_H and g_H instead of f_E and g_E , respectively, in the above. In (A1)-(A7), the integrals are given by

$$a_{mn,f}^{pq} = \frac{1}{4\pi} \int_S \mathbf{f}_m^p(\mathbf{r}) \cdot \int_S \frac{\mathbf{f}_n^q(\mathbf{r}')}{R} dS' dS, \quad (\text{A8})$$

$$a_{mn,g}^{pq} = \frac{1}{4\pi} \int_S \mathbf{g}_m^p(\mathbf{r}) \cdot \int_S \frac{\mathbf{f}_n^q(\mathbf{r}')}{R} dS' dS, \quad (\text{A9})$$

$$b_{mn,f}^{pq} = \frac{1}{4\pi} \int_S \nabla' \cdot \mathbf{f}_m^p(\mathbf{r}) \int_S \frac{\nabla' \cdot \mathbf{f}_n^q(\mathbf{r}')}{R} dS' dS, \quad (\text{A10})$$

$$f_{mn,g}^{pq} = \frac{1}{4\pi} \int_S \mathbf{g}_m^p(\mathbf{r}) \cdot \int_S \nabla' \cdot \mathbf{f}_n^q(\mathbf{r}') \frac{\hat{\mathbf{R}}}{R} dS' dS, \quad (\text{A11})$$

$$g_{mn,g}^{pq} = \frac{1}{4\pi} \int_S \mathbf{g}_m^p(\mathbf{r}) \cdot \int_S \nabla' \cdot \mathbf{f}_n^q(\mathbf{r}') \frac{\hat{\mathbf{R}}}{R^2} dS' dS, \quad (\text{A12})$$

$$c_{mn,f}^{pq} = \frac{1}{2} \int_S \mathbf{f}_m^p(\mathbf{r}) \cdot \mathbf{n} \times \mathbf{f}_n^q(\mathbf{r}) dS, \quad (\text{A13})$$

$$c_{mn,g}^{pq} = \frac{1}{2} \int_S \mathbf{g}_m^p(\mathbf{r}) \cdot \mathbf{n} \times \mathbf{f}_n^q(\mathbf{r}) dS, \quad (\text{A14})$$

$$d_{mn,f}^{pq} = \frac{1}{4\pi} \int_S \mathbf{f}_m^p(\mathbf{r}) \cdot \int_S \mathbf{f}_n^q(\mathbf{r}') \times \frac{\hat{\mathbf{R}}}{R} dS' dS, \quad (\text{A15})$$

$$d_{mn,g}^{pq} = \frac{1}{4\pi} \int_S \mathbf{g}_m^p(\mathbf{r}) \cdot \int_S \mathbf{f}_n^q(\mathbf{r}') \times \frac{\hat{\mathbf{R}}}{R} dS' dS, \quad (\text{A16})$$

$$e_{mn,f}^{pq} = \frac{1}{4\pi} \int_S \mathbf{f}_m^p(\mathbf{r}) \cdot \int_S \mathbf{f}_n^q(\mathbf{r}') \times \frac{\hat{\mathbf{R}}}{R^2} dS' dS, \quad (\text{A17})$$

$$e_{mn,g}^{pq} = \frac{1}{4\pi} \int_S \mathbf{g}_m^p(\mathbf{r}) \cdot \int_S \mathbf{f}_n^q(\mathbf{r}') \times \frac{\hat{\mathbf{R}}}{R^2} dS' dS, \quad (\text{A18})$$

where $\hat{\mathbf{R}}$ is a unit vector along the direction $\mathbf{r} - \mathbf{r}'$. The evaluation of (A8)-(A18) has been presented in [11]-[18]. The integrals associated with the incident field are expressed as

$$V_m^{E(v)}(t) = \begin{cases} \int_S [f_E \mathbf{f}_m(\mathbf{r}) + g_E \mathbf{g}_m(\mathbf{r}) \cdot \mathbf{E}^i(\mathbf{r}, t)] dS, & v=1, \\ 0, & v=2, \end{cases} \quad (\text{A19})$$

$$V_m^{H(v)}(t) = \begin{cases} \int_S [f_H \mathbf{f}_m(\mathbf{r}) + g_H \mathbf{g}_m(\mathbf{r}) \cdot \mathbf{H}^i(\mathbf{r}, t)] dS, & v=1, \\ 0, & v=2. \end{cases} \quad (\text{A20})$$

References

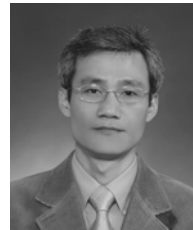
- [1] S.M. Rao, *Time Domain Electromagnetics*, Academic Press, 1999.
- [2] D.A. Vechinski, S.M. Rao, and T.K. Sarkar, "Transient Scattering from Three-Dimensional Arbitrary-Shaped Dielectric Bodies," *J. Opt. Soc. Amer.*, vol. 11, no. 4, Apr. 1994, pp. 1458-1470.
- [3] S.M. Rao and T.K. Sarkar, "Implicit Solution of Time-Domain Integral Equations for Arbitrarily Shaped Dielectric Bodies," *Microwave Opt. Technol. Lett.*, vol. 21, no. 3, May 1999, pp. 201-205.
- [4] T.K. Sarkar, W. Lee, and S.M. Rao, "Analysis of Transient Scattering from Composite Arbitrarily Shaped Complex Structures," *IEEE Trans. Antennas Propagat.*, vol. 48, no. 10, Oct. 2000, pp. 1625-1634.
- [5] B.H. Jung, T.K. Sarkar, Y.S. Chung, Z. Ji, and M. Salazar-Palma, "Analysis of Transient Electromagnetic Scattering from Dielectric Objects Using a Combined-Field Integral Equation," *Microwave Opt. Technol. Lett.*, vol. 40, no. 6, Mar. 2004, pp. 476-481.
- [6] X.Q. Sheng, J.M. Jin, J.M. Song, W.C. Chew, and C.C. Lu, "Solution of Combined-Field Integral Equation Using Multilevel Fast Multipole Algorithm for Scattering by Homogeneous Bodies," *IEEE Trans. Antennas Propagat.*, vol. 46, no. 11, Nov.

1998, pp. 1718-1726.

- [7] B.H. Jung, T.K. Sarkar, and Y.S. Chung, "A Survey of Various Frequency Domain Integral Equations for the Analysis of Scattering from Three-Dimensional Dielectric Objects," *J. of Electromagn. Waves and Applicat.*, vol. 16, no. 10, 2002, pp. 1419-1421.
- [8] B.H. Jung, Y.S. Chung, and T.K. Sarkar, "Time-Domain EFIE, MFIE, and CFIE Formulations Using Laguerre Polynomials as Temporal Basis Functions for the Analysis of Transient Scattering from Arbitrary Shaped Conducting Structures," *J. of Electromagn. Waves and Applicat.*, vol. 17, no. 5, 2003, pp. 737-739.
- [9] S.M. Rao, D.R. Wilton, and A.W. Glisson, "Electromagnetic Scattering by Surfaces of Arbitrary Shape," *IEEE Trans. Antennas Propagat.*, vol. 30, no. 3, May 1982, pp. 409-418.
- [10] A.D. Poularikas, *The Transforms and Applications Handbook*, IEEE Press, 1996.
- [11] S.M. Rao, *Electromagnetic Scattering and Radiation of Arbitrarily Shaped Surfaces by Triangular Patch Modeling*, PhD Dissertation, Univ. Mississippi, Aug. 1980.
- [12] D.R. Wilton, S.M. Rao, A.W. Glisson, D.H. Schaubert, O.M. Al-Bundak, and C.M. Butler, "Potential Integrals for Uniform and Linear Source Distributions on Polygonal and Polyhedral Domains," *IEEE Trans. Antennas Propagat.*, vol. 32, no. 3, Mar. 1984, pp. 276-281.
- [13] R.D. Graglia, "Static and Dynamic Potential Integrals for Linearly Varying Source Distributions in Two- and Three-Dimensional Problems," *IEEE Trans. Antennas Propagat.*, vol. 35, no. 6, June 1987, pp. 662-669.
- [14] S. Caorsi, D. Moreno, and F. Sidoti, "Theoretical and Numerical Treatment of Surface Integrals Involving the Free-Space Green's Function," *IEEE Trans. Antennas Propagat.*, vol. 41, no. 9, Sep. 1993, pp. 1296-1301.
- [15] R.D. Graglia, "On the Numerical Integration of the Linear Shape Functions Times the 3-D Green's Function or its Gradient on a Plane Triangle," *IEEE Trans. Antennas Propagat.*, vol. 41, no. 10, Oct. 1993, pp. 1448-1455.
- [16] T.F. Eibert and V. Hansen, "On the Calculation of Potential Integrals for Linear Source Distributions on Triangular Domains," *IEEE Trans. Antennas Propagat.*, vol. 43, no. 12, Dec. 1995, pp. 1499-1502.
- [17] R.E. Hodges and Y. Rahmat-Samii, "The Evaluation of MFIE Integrals with the Use of Vector Triangle Basis Functions," *Microwave Opt. Technol. Lett.*, vol. 14, no. 1, Jan. 1997, pp. 9-14.
- [18] P. Yla-Oijala and M. Taskinen, "Calculation of CFIE Impedance Matrix Elements with RWG and $n \times$ RWG Functions," *IEEE Trans. Antennas Propagat.*, vol. 51, no. 8, Aug. 2003, pp. 1837-1846.



Young-Hwan Lee received the BS in electronic engineering from Soongsil University, Seoul, Korea, in 1984, and the MS in electronic engineering from Kwangwoon University, Seoul, Korea, in 1986. He received the PhD degree from the Information and Communications University, Daejeon, Korea, in 2007. Since July 1989, he has been with the Wireless Communications Technical Regulation Section at the Electronics and Telecommunication Research Institute (ETRI), Daejeon, Korea, where he is currently a Principle Member of Research Staff. His current research interests include electromagnetics and wave propagation, wireless communication standards, antenna theory, and radio regulation.



Baek Ho Jung received the BS, MS, and PhD degrees in electronic and electrical engineering from Kyungpook National University, Taegu, Korea, in 1986, 1989, and 1997, respectively. From 1989 to 1994, he was a Researcher with the Agency for Defense Development in Korea. Since 1997, he has been a Lecturer and is currently an Associate Professor with the Department of Information and Communication Engineering, Hoseo University, Asan, Chungnam, Korea. He was a Visiting Scholar with Syracuse University, Syracuse, NY, from 2001 to 2003. His current research interests are computational electromagnetics and wave propagation.



Tapan K. Sarkar received the BTech degree from the Indian Institute of Technology, Kharagpur, in 1969, the MScE degree from the University of New Brunswick, Fredericton, NB, Canada, in 1971, and the MS and PhD degrees from Syracuse University, Syracuse, NY, in 1975. From 1975 to 1976, he was with the TACO Division of the General Instruments Corporation. He was with the Rochester Institute of Technology, Rochester, NY, from 1976 to 1985. He was a Research Fellow at the Gordon McKay Laboratory, Harvard University, Cambridge, MA, from 1977 to 1978. He is now a Professor in the Department of Electrical and Computer Engineering, Syracuse University and concurrently the President of OHRN Enterprises, a small business established in 1985 in New York State to implement various theories to the solution of various challenging electromagnetic and signal processing problems. His current research interests deal with numerical solutions of operator equations arising in electromagnetics and signal processing with application to system design. He has authored or coauthored more than 280 journal articles, numerous conference papers, 32 chapters in books, and 15 books, including his most recent ones, *History of Wireless* (John Wiley & Sons, 2005), *Smart Antennas* (John Wiley & Sons, 2003), *Wavelet Applications in Electromagnetics and Signal Processing* (Boston, MA, Artech House, 2002), and *Iterative and Self-Adaptive Finite-Elements in Electromagnetic Modeling* (Boston, MA, Artech House, 1998).



Mengtao Yuan was born in Chongqing, China. He received the BS degree in information and electronic engineering and the MS degree in information and communication system from Zhejiang University, China, in 1999 and 2002, respectively, and his PhD degree in electrical engineering at Syracuse University, in 2006. He

was a Research Assistant at Syracuse University from 2002 to 2006. He is now a Senior Member of Technical Staff with Cadence Design Systems, Inc., Tempe, Arizona. His current research interests include electromagnetic simulation in multi-layered media, the time and frequency domain computational electromagnetic efficient solver for electrically large structures, circuit and antenna design, and signal processing in communications.



Zhong Ji received both BS and MS degrees from Shandong University, China, in 1988 and 1991, respectively. He received the PhD degree from Shanghai Jiao Tong University, China, in 2000. From 1971 to 1997, he was a teacher with Shandong University, Jinan, China. From 2000 to 2005, he was an Research Associate at

Syracuse University, Syracuse, NY. He is now a RF Antenna Engineer with Laird Technologies, Lincoln, NE. His current research interests deal with antenna design and antenna integration for wireless devices.



Seong-Ook Park was born in Gyeongbuk, Korea, on December, 1964. He received the BS degree from Gyeongbuk National University, KyungPook, Korea, in 1987, the MS degree from Korea Advanced Institute of Science and Technology, Seoul, Korea, in 1989, and the PhD degree from Arizona State University, Tempe,

AZ, in 1997, all in electrical engineering. From March 1989 to August 1993, he was an Research Engineer with Korea Telecom, Daejeon, Korea, working with microwave systems and networks. He later joined the Telecommunication Research Center, Arizona State University, until his departure in September 1997. Since October 1997, he has been with the Information and Communications University, Daejeon, Korea, as an Assistant Professor. Currently, he is an Associate Professor. His research interests include 4G handset antennas, mm/mw systems, and analytical and numerical techniques in the area of electromagnetics. Dr. Park is a Member of Phi Kappa Phi Scholastic Honor Societies.